

QTrack: Query-Driven Reasoning for Multi-modal MOT

Tajamul Ashraf^{1,4*}, Tavaheed Tariq^{4†}, Sonia Yadav^{4†}, Abrar Ul Riyaz⁴, Wasif Tak^{2‡}, Moloud Abdar³, and Janibul Bashir⁴

¹ King Abdullah University of Science and Technology (KAUST), Saudi Arabia

² Thapar Institute of Engineering and Technology, India

³ The University of Queensland, Australia

⁴ Gaash Research Lab, National Institute of Technology Srinagar, India

Project Page: <https://gaashlab.github.io/QTrack/>

Abstract. Multi-object tracking (MOT) has traditionally focused on estimating trajectories of all objects in a video, without selectively reasoning about user-specified targets under semantic instructions. In this work, we introduce a query-driven tracking paradigm that formulates tracking as a spatiotemporal reasoning problem conditioned on natural language queries. Given a reference frame, a video sequence, and a textual query, the goal is to localize and track only the target(s) specified in the query while maintaining temporal coherence and identity consistency. To support this setting, we construct **RMOT26**, a large-scale benchmark with grounded queries and sequence-level splits to prevent identity leakage and enable robust generalization evaluation. We further present **QTrack**, an end-to-end vision language model that integrates multi-modal reasoning with tracking-oriented localization. Additionally, we introduce a Temporal Perception-Aware Policy Optimization strategy with structured rewards to encourage motion-aware reasoning. Extensive experiments demonstrate the effectiveness of our approach for reasoning-centric, language-guided tracking. Code and data are available at <https://github.com/gaash-lab/QTrack>

Keywords: Multi-Object Tracking · Vision-Language Models · Spatiotemporal Reasoning · Reinforcement Learning

1 Why Query-Driven Tracking?

Multi-object tracking (MOT) is a fundamental computer vision task that aims to detect and consistently associate multiple objects across frames temporally [49]. Given a video, traditional MOT methods [7, 28, 37] primarily aim to estimate the trajectories of all moving objects, i.e., answering “*what are the locations*

*Corresponding author: tajamul.ashraf@kaust.edu.sa

†These authors contributed equally.

‡Work done while an intern at Gaash Lab, NIT Srinagar

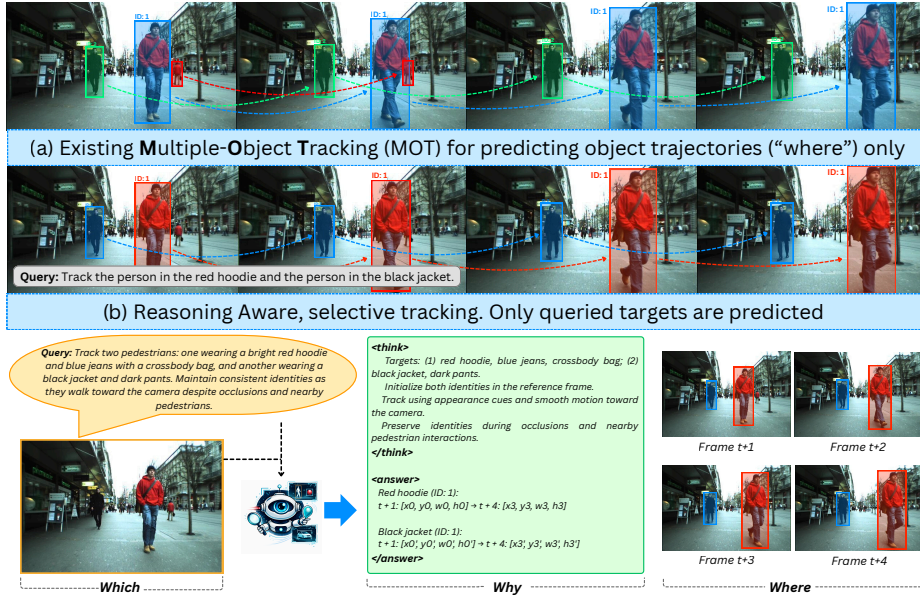


Fig. 1: Comparison of tracking paradigms. (a) Traditional MOT follows a tracking-by-detection paradigm, tracking all objects from predefined categories regardless of user intent. (b) QTrack enables reasoning-aware, query-conditioned tracking: given a video and natural language query, it selectively identifies and tracks only the specified targets, shifting from all-object tracking to semantic, user-driven tracking.

and identities of objects over time?”. These approaches operate at the category level with predefined classes and are not designed for query-specific, language-conditioned tracking of a particular target. Despite considerable advancements in the deep learning era [12, 39, 43], focusing solely on spatial localization in existing MOT frameworks is insufficient for comprehensive video understanding in many real-world applications. For example, beyond estimating trajectories, understanding trajectory-associated semantic⁵ attributes such as the identity, role, or contextual relevance of a queried target is crucial for real-world applications like surveillance and robotics. For instance, consider a crowded street scene where multiple individuals wear similar clothing. A query such as “track the person who picks up the red backpack and later enters the taxi” cannot be solved through appearance similarity alone. The model must reason about temporally evolving actions and maintain identity consistency even when the target undergoes occlusion or appearance changes. This motivates extending conventional MOT (addressing “where”) toward query-conditioned tracking that jointly reasons about “which” target to follow based on semantic instructions.

⁵Here, by “semantic”, we refer to high-level, trajectory-based activity understanding in videos within the context of tracking, rather than category-level labeling as in semantic segmentation.

In parallel, vision-language models (VLMs) have demonstrated remarkable capabilities in multi-modal grounding [59, 72], visual reasoning [3, 54, 64], and following [17, 76]. By aligning visual representations with natural language semantics, VLMs enable fine-grained instance understanding beyond category-level perception. While prior works on referring video object segmentation and language-guided tracking focus on grounding a static description to a target instance, they often treat tracking and reasoning as loosely coupled modules. These systems do not explicitly leverage semantic queries to guide identity persistence, motion prediction, or occlusion recovery.

Motivated by these limitations, we introduce **QTrack**, a query-centric tracking paradigm that extends conventional MOT beyond trajectory estimation toward language-conditioned, target-specific reasoning. Unlike traditional MOT methods that focus solely on predicting object trajectories (“where”), this paradigm enables tracking of objects specified through natural language queries, integrating spatial localization with semantic grounding. Given a video, a reference grounding, and a query (e.g., “track the person wearing a red jacket”), the model identifies and persistently tracks only the specified instance across frames. This requires joint reasoning over appearance, motion dynamics, contextual cues, and temporal continuity, emphasizing *which* object to follow and *why*, rather than indiscriminately tracking all category-level instances. By unifying “where” (trajectory estimation) with “which” (query-grounded selection), the framework advances tracking from passive perception to reasoning-aware, language-guided video understanding.

To realize this paradigm, we develop a reinforcement learning-optimized vision–language framework for temporally consistent, query-conditioned object localization. Given a video and a query, the model generates structured reasoning and directly predicts bounding boxes for the queried targets in an end-to-end manner. Unlike detect-then-track pipelines or loosely coupled vision–language systems, our approach jointly optimizes grounding and temporal consistency. Specifically, we introduce Temporal Perception-Aware Policy Optimization (TAPO), which incorporates temporal corruption and KL-based regularization to encourage motion-aware reasoning and identity persistence. While standard supervised training optimizes frame-level localization losses and may suffer from identity drift under long-term dependencies, our reinforcement learning formulation directly optimizes sequence-level objectives, promoting coherent motion dynamics and robust identity preservation across frames.

To facilitate research on query-driven tracking with reasoning, we introduce **RMOT26**, which consists of a diverse collection of real-world video sequences spanning crowded scenes, sports, complex interactions, non-linear motion, and severe occlusions. Each sample is paired with (i) a *reference frame* with explicit spatial grounding of the target instance and (ii) a *natural-language query* specifying the tracking objective (e.g., identity, attributes, role, or context). Unlike conventional MOT benchmarks that evaluate category-level tracking of all objects, **RMOT26** explicitly tests a model’s ability to *reason* about *which* instance to follow and to maintain identity persistence under appearance ambiguity, long-term

temporal dependencies, and occlusion recovery. We design multiple query types to probe single-target tracking, multi-target reasoning, and occlusion-aware re-identification, with strong spatial and temporal supervision derived from high-quality verified annotations. All splits are performed at the *sequence level* to prevent identity leakage and ensure robust generalization.

Despite its streamlined design, **QTrack** demonstrates strong performance in language-guided tracking scenarios and significantly outperforms baselines that combine tracking and VLM reasoning in an offline manner, highlighting the effectiveness of reinforcement learning-driven spatiotemporal reasoning. In summary, our contributions are:

- We introduce **QTrack**, a novel query-driven, reasoning-centric tracking paradigm that advances MOT from passive trajectory prediction to language-conditioned spatiotemporal reasoning, enabled by our Temporal Perception-Aware Policy Optimization (TAPO) and structured reward design.
- We construct RMOT26, a large-scale benchmark with grounded natural language queries and temporally consistent supervision to systematically evaluate reasoning-aware tracking.
- We demonstrate strong performance and provide in-depth analysis on 10+ VLM baselines to guide future research on reasoning-aware, multimodal tracking systems.

2 Related Work

2.1 Tracking and Language-Guided Grounding

Benchmarks have played a critical role in advancing MOT, from early datasets such as PETS2009 [19] to the MOT Challenge series [15, 16, 29, 40]. Domain-specific benchmarks include KITTI [60] and BDD100K [71] for autonomous driving, ImageNet-VID [24] and TAO [14] for large-scale and long-tail tracking, DanceTrack [52] and SportsMOT [13] for articulated human motion, AnimalTrack [73] for wildlife tracking, and UAVDT [25] and VisDrone [77] for drone scenarios. Despite their diversity, these datasets evaluate trajectory prediction alone (“where”), without incorporating semantic or query-conditioned reasoning. Methodologically, classical MOT follows the tracking-by-detection paradigm [8, 65], later unified with re-identification in FairMOT [74]. Recent advances include Tracking-by-Detection approaches [5, 9, 10, 53], Joint Detection-and-Tracking frameworks [], and Transformer-based trackers [6, 43, 58, 78], all primarily improving trajectory estimation. While effective, these methods remain task-agnostic, tracking all category-level instances without conditioning on semantic context. Language-guided tracking introduces natural language as a target specifier [30, 62], and multi-object extensions such as LaMOT [32] expand to multiple referred entities. Referring video object segmentation and grounding methods [18, 20, 66] further strengthen language–video alignment, but remain limited to grounding specified objects rather than reasoning over multiple candidates conditioned on a

question. In contrast, RMOT26 requires *question-conditioned multi-object grounding and temporal identity tracking*, jointly modeling localization and trajectory-aware semantic reasoning.

2.2 Video Reasoning and Vision Language Models

Unlike video captioning [1, 26, 41, 46, 50, 61], which generates global natural language descriptions of video content, RMOT26 focuses on language comprehension grounded in dense multi-object trajectories, requiring precise temporal identity tracking alongside fine-grained semantic reasoning. Video question answering (VideoQA) benchmarks such as TGIF-QA [27], NExT-QA [68], and AGQA [22] emphasize spatio-temporal reasoning over actions, events, and object relations. However, these datasets evaluate only final textual answers without requiring explicit trajectory outputs, enabling models to rely on global cues or dataset priors. In contrast, RMOT26 *externalizes* reasoning by requiring models to generate question-relevant object trajectories as structured spatiotemporal evidence. Large vision language models (VLMs), including CLIP [44] and video-enabled architectures such as Flamingo [4], have demonstrated strong open-vocabulary grounding and multimodal reasoning capabilities. However, they lack explicit identity-preserving temporal modeling and do not natively support structured multi-object tracking. Reinforcement learning has recently become a powerful paradigm for improving reasoning in large language models, with approaches such as RLHF [42], DPO [45], and PPO [47]. More recently, DeepSeek-R1 [23] leveraged Group Relative Policy Optimization (GRPO) [48] to enhance test-time reasoning and scaling behavior. Inspired by these advances, reinforcement learning techniques have begun to extend to large vision language models, including Visual-RFT [36], EasyR1 [75], and Seg-Zero [34] and PAPO [63] (Perception-Aware Policy Optimization) incorporate perception-aligned reward shaping to ensure that reasoning remains grounded in reliable visual evidence. Building upon this line of work, our **QTrack** framework integrates VLM grounding with structured trajectory formation and temporal reasoning, optimized via GRPO and our proposed Temporal Perception-Aware Policy Optimization (TAPO). This unified reinforcement learning design enables explicit, interpretable, question-conditioned multi-object tracking with identity consistency across time.

3 Methodology

To develop a unified query-driven tracking framework capable of reasoning over spatiotemporal dynamics, we first formalize the reasoning-based multi-object tracking task and categorize its input-output structure. We then describe the architecture of our **QTrack** framework, which integrates multimodal reasoning with tracking-oriented localization (Section 3.3). Next, we introduce our structured reward design, including motion-aware supervision and temporal consistency constraints (Section 3.4). Finally, we detail our reinforcement learning training strategy based on GRPO and the proposed Temporal Perception-

Aware Policy Optimization (TAP0) for motion-sensitive policy optimization (Section 3.5).

3.1 Preliminaries

Conventional MOT models vs. VLMs Traditional multi-object tracking (MOT) methods are primarily designed for closed-set perception, focusing on detecting and associating objects from predefined categories across frames. While these approaches achieve strong performance on standard benchmarks, they operate at the category level and are limited to answering “where objects are located”, without modeling semantic intent or query-specific selection. As a result, they struggle to handle open-ended, attribute-based, or compositional instructions that specify a particular instance among multiple candidates. In contrast, large vision language models (VLMs) align visual representations with natural language semantics, enabling flexible grounding of free-form queries. This capability is essential for query-driven tracking, where the objective is not to track all objects, but to identify and persistently follow a semantically specified target. Integrating VLM reasoning into MOT allows the tracking process to move beyond category-level association toward identity-aware and language-conditioned spatiotemporal reasoning.

Group Relative Policy Optimization (GRPO). To enable structured reasoning and trajectory prediction in **QTrack**, we adopt Group Relative Policy Optimization (GRPO), an on-policy reinforcement learning algorithm that stabilizes policy updates through relative reward comparison across sampled rollouts. Unlike conventional supervised training that optimizes frame-level localization losses independently, our setting requires optimizing sequence-level reasoning quality and long-term identity consistency. These objectives are difficult to encode through differentiable losses alone, especially when reasoning traces and trajectory formation are jointly generated. Reinforcement learning allows us to directly optimize structured, sequence-level rewards that reflect spatial accuracy, motion coherence, and reasoning validity in a unified objective. In our setting, the policy π_θ generates structured reasoning traces and corresponding bounding box trajectories conditioned on the video frames and the query.

Given an input $x = (\mathcal{F}, q)$ consisting of a frame sequence \mathcal{F} and a natural language query q , the previous policy $\pi_{\theta_{\text{old}}}$ produces a group of rollouts $\{o_i\}_{i=1}^G$. Each rollout contains a chain-of-thought reasoning trace along with predicted bounding boxes for the queried targets. A task-specific reward function evaluates each rollout and assigns scalar rewards $\{r_i\}_{i=1}^G$ based on spatial accuracy, motion consistency, and structured output validity.

To reduce reward variance and emphasize relative performance within the sampled group, we compute a normalized relative advantage:

$$A_i = \frac{r_i - \text{mean}(\{r_1, r_2, \dots, r_G\})}{\text{std}(\{r_1, r_2, \dots, r_G\})}. \quad (1)$$

The policy is then updated by maximizing a clipped surrogate objective:

$$J_{\text{GRPO}}(\theta) = \mathbb{E}_{x \sim \mathcal{D}, \{o_i\} \sim \pi_{\theta_{\text{old}}}} \left[\frac{1}{G} \sum_{i=1}^G \min \left(\frac{\pi_{\theta}(o_i | x)}{\pi_{\theta_{\text{old}}}(o_i | x)} A_i, \text{clip} \left(\frac{\pi_{\theta}(o_i | x)}{\pi_{\theta_{\text{old}}}(o_i | x)}, 1 - \epsilon, 1 + \epsilon \right) A_i \right) - \beta D_{KL}(\pi_{\theta} \| \pi_{\text{ref}}) \right], \quad (2)$$

where ϵ controls policy clipping and β regularizes deviation from a reference policy π_{ref} to prevent instability.

Compared to PPO, GRPO stabilizes learning by computing relative advantages across multiple rollouts of the same input, emphasizing better reasoning trajectories while reducing reward variance under structured, high-variability outputs.

3.2 Task Reformulation for Query-Driven Tracking

We analyze query-conditioned tracking tasks and observe that they can be reformulated into three fundamental spatiotemporal reasoning types. Unlike static perception problems, **QTrack** operates over video sequences and requires joint spatial grounding and temporal identity modeling.

Spatial Grounding. Given a video sequence $\mathcal{V} = \{I_t\}_{t=1}^T$ and a natural language query q , the spatial grounding task aims to localize the queried target(s) in specific frames by predicting bounding boxes $\{b_i^t\}$. This corresponds to instance-level detection conditioned on semantic instructions. It requires identifying candidate objects based on attributes, roles, or contextual descriptions provided in the query.

Temporal Tracking. Beyond frame-level localization [69, 70], the temporal tracking task requires associating predictions across frames to form coherent trajectories $\{\tau_i\}$. This involves modeling motion dynamics, maintaining identity persistence, and handling occlusion or appearance variation over time. Unlike traditional MOT, which tracks all category-level objects [32, 65, 74], **QTrack** tracks only the query-specified targets.

Relational and Reasoning-Based Tracking. Certain queries require reasoning over interactions, comparisons, or multi-object relations (e.g., selecting an object based on its behavior or relationship with others). This task type requires compositional reasoning over both spatial and temporal cues before trajectory formation. It extends tracking from passive localization to question-conditioned decision-making.

Together, these three components, spatial grounding, temporal association, and relational reasoning form the foundation of query-driven spatiotemporal tracking in RMOT26. This reformulation highlights that **QTrack** is not merely a trajectory prediction problem, but a structured reasoning task over dynamic visual scenes. This decomposition is not merely descriptive; it guides the architectural and reward design of **QTrack**. Spatial grounding informs the localization objective, temporal tracking motivates motion-aware supervision, and relational reasoning necessitates structured policy learning capable of compositional decision-making.

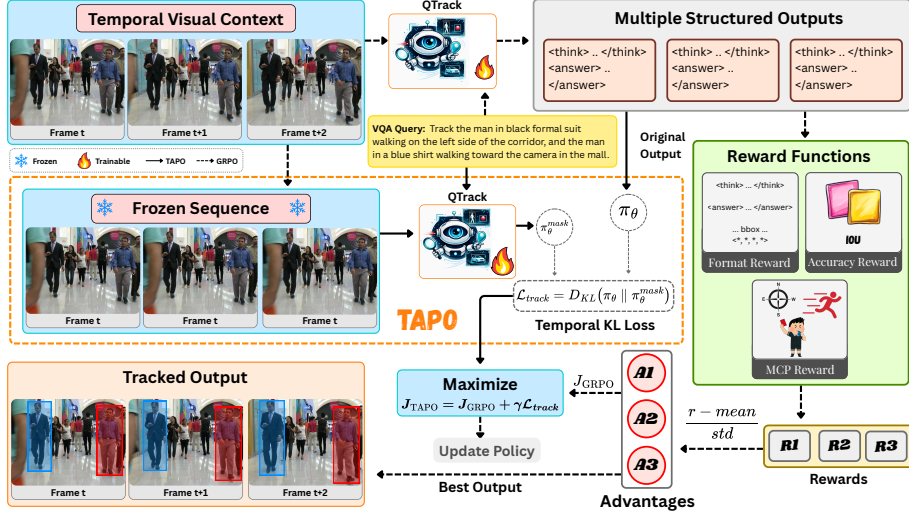


Fig. 2: Overview of the QTrack Framework architecture. Given an input video sequence $\mathcal{V} = \{I_t\}_{t=1}^T$ and natural-language query q . QTrack processes the data through a unified vision-language model (VLM). The model first generates a chain-of-thought reasoning trace, analyzing the query in the context of a visual scene to identify targets based on attributes, relationship or motion. The model directly predicts bounding box trajectories $\{\tau_i\}_{i=1}^{N_q}$ for the queried target across all frames, performing joint spatial grounding and temporal association.

3.3 QTrack Framework

Our framework incorporates a reasoning module for query-conditioned spatiotemporal grounding and a tracking-oriented localization module for trajectory formation. The overall architecture is illustrated in Figure 2. The key strength of **QTrack** lies in its ability to perform multi-object reasoning over video sequences, enabling unified spatial grounding, temporal association, and identity persistence under natural language instructions.

Specifically, given a video sequence $\mathcal{V} = \{I_t\}_{t=1}^T$ and a text query q , **QTrack** first generates an interpretable reasoning trace that identifies candidate targets based on semantic attributes, contextual cues, and motion patterns. The model then predicts structured bounding boxes $\{b_i^t\}$ corresponding to the queried targets across frames. These predictions are aggregated to form trajectories $\{\tau_i\}_{i=1}^{N_q}$. This process can be formulated as: $\{\tau_i\}_{i=1}^{N_q} = F(\mathcal{V}, q)$, where F denotes the **QTrack** policy that jointly reasons over spatial and temporal cues. During inference, the user provides a video \mathcal{V} and a natural language query q . The system outputs trajectories corresponding only to the query-relevant objects:

$$\text{Output} = \begin{cases} \{\tau_i\}_{i=1}^{N_q}, & \text{if query specifies one or multiple targets,} \\ \emptyset, & \text{if no valid target satisfies the query.} \end{cases} \quad (3)$$

Unlike traditional MOT, which tracks all detected objects, **QTrack** selectively tracks only those instances grounded in the query. By integrating reasoning and trajectory prediction within a unified framework, **QTrack** extends multi-object tracking from passive category-level perception to question-conditioned, identity-preserving spatiotemporal reasoning.

3.4 Unified Reward Mechanism for QTrack

As discussed in Section 3.1, reward design is central to group-relative reinforcement learning. In **QTrack**, we employ a unified reward mechanism tailored for query-conditioned multi-object tracking, jointly enforcing structured reasoning, spatial accuracy, and temporal motion consistency. The total reward is the sum of all components.

Thinking Format Reward. Assigns 1.0 if the reasoning trace is enclosed within `<think>` and `</think>` tags and the final prediction appears within `<answer>` and `</answer>` tags.

Answer Format Reward. Ensures bounding boxes follow the predefined JSON format: `[{'bbox_2d' : [x1, y1, x2, y2]}, ...]`. Reward is 1.0 for valid format, otherwise 0.

IoU Reward. After Hungarian matching between predicted boxes $\{b_i^{pred}\}_{i=1}^K$ and ground-truth boxes $\{b_j^{gt}\}_{j=1}^N$, each matched pair with IoU > 0.5 contributes $\frac{1}{\max(K, N)}$.

Motion Consistency Precision (MCP) Reward. Evaluates trajectory dynamics via direction alignment (cosine similarity), speed consistency (Gaussian penalty), and anti-static penalty. The final MCP score is the product of these components in $[0, 1]$, thereby enforcing temporally coherent motion patterns.

For multi-object cases, spatial and motion rewards are computed using batch matching with the Hungarian algorithm to ensure optimal one-to-one alignment.

Note that the format-related rewards serve as auxiliary regularizers to ensure structured and parsable outputs during early training stages. They do not directly influence localization quality but improve optimization stability in VLMs. A detailed description of reward functions is provided in Appendix §C.

Algorithm 1 TAPO: Temporal Perception-Aware Optimization

- 1: **Input:** Video $\mathcal{F} = (F_0, \dots, F_T)$, query q , policy π_θ , weight γ
 - 2: Generate rollout $o \sim \pi_\theta(o | q, \mathcal{F})$
 - 3: Construct corrupted sequence \mathcal{F}^{mask}
 - 4: Freeze frames: $\tilde{F}_t = F_0$
 - 5: Compute log-probabilities:
 - 6: $\log p = \log \pi_\theta(o | q, \mathcal{F})$
 - 7: $\log p^{mask} = \log \pi_\theta(o | q, \mathcal{F}^{mask})$
 - 8: Compute temporal loss:
 - 9: $\mathcal{L}_{track} = \log p - \log p^{mask}$
 - 10: $J = J_{grpo} + \gamma \mathcal{L}_{track}$
 - 11: Update θ using J
-

3.5 Temporal Perception-Aware Policy Optimization (TAPO)

While GRPO improves the quality of the reasoning, we empirically observe that, without additional temporal regularization, the policy may over-rely on static

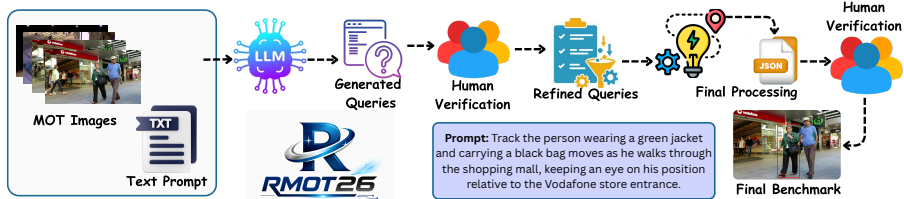


Fig. 3: RMOT26 dataset construction pipeline. This pipeline explains the creation of benchmark instances from existing MOT datasets.

appearance cues and ignore motion dynamics, especially in crowded scenes with similar visual attributes. Such behavior leads to identity drift under occlusion or viewpoint changes. To address this, we introduce Temporal Perception-Aware Policy Optimization (TAPO), summarized in Algorithm 1.

Temporal Corruption. Given a video sequence $\mathcal{F} = (F_0, F_1, \dots, F_T)$, we construct a corrupted sequence \mathcal{F}^{mask} by freezing frames: $F_t^{mask} = F_0, \forall t$. This removes motion while preserving static appearance.

Temporal KL Loss. We enforce temporal sensitivity by computing a divergence between policy outputs under original and corrupted sequences, as detailed in Algorithm 1:

$$\mathcal{L}_{track} = D_{KL}(\pi_{\theta}(o | q, \mathcal{F}) \| \pi_{\theta}(o | q, \mathcal{F}^{mask})). \quad (4)$$

We adopt this asymmetric KL formulation to explicitly penalize policies whose predictions remain invariant under temporal corruption. By measuring divergence from the original motion-aware policy to the corrupted-input policy, we directly discourage motion-agnostic behavior while preserving stable reference outputs.

Overall Objective. The final optimization objective combines GRPO reward and temporal perception regularization:

$$J_{TAPO} = J_{GRPO} + \gamma \mathcal{L}_{track}, \quad (5)$$

where γ controls the strength of temporal enforcement. Together, the structured reward design, MCP motion supervision, and TAPO regularization adapt GRPO to query-conditioned, identity-preserving multi-object tracking.

4 RMOT26 Benchmark

Dataset Design. The proposed RMOT26 benchmark is designed to evaluate fine-grained, query-conditioned spatiotemporal reasoning in realistic multi-object tracking scenarios. We curate video clips from seven popular MOT datasets, including DanceTrack [52], MOT16/17 [29, 40], MOT20 [16], SportsMOT [13], PETS [19], TAO [14], and DAMUNT [2]. These datasets span diverse motion patterns, crowd densities, camera viewpoints, and scene dynamics, including

non-linear motion (DanceTrack), fast sports interactions (SportsMOT), crowded surveillance scenes (MOT16/17/20), and static camera footage with heavy overlaps (PETS). This diversity ensures evaluation beyond static grounding toward motion-aware reasoning. Each instance consists of a reference frame and a short sequence of future frames (5–6 frames). Target objects are grounded in the reference frame via bounding boxes, while subsequent frames test trajectory prediction and motion reasoning. Object identities are inherited from the original MOT annotations, ensuring consistent track IDs across frames. The overall dataset construction pipeline is illustrated in Fig. 3.

Query Types and Reasoning Categories. Each benchmark instance includes a natural language query derived from MOT annotations, paired with explicit spatial grounding in the reference frame. We define three query categories: *Single-Object Queries*: Track a specified object from the reference frame across future frames, producing a sequence of bounding boxes corresponding to its trajectory. *Multi-Object Queries*: Simultaneously track multiple referenced objects, each defined by bounding boxes and textual descriptions in the reference frame. The output consists of structured trajectories for all specified targets. *Occlusion-Aware Queries*: Track objects that are partially or fully occluded in the reference frame but visible in later frames, requiring identity persistence under visibility changes. All queries are tightly grounded spatially through explicit bounding boxes in the reference frame, eliminating ambiguity in object selection.

Annotation Protocol. Trajectory supervision is derived directly from ground-truth MOT annotations. For each query, bounding boxes of referenced objects are extracted across subsequent frames to form ordered trajectories indexed by frame number. Single-object queries require a trajectory array, while multi-object queries require a structured mapping between object identities and their tracks. Each query includes: (1) a natural language description of the target object(s), (2) explicit bounding boxes in the reference frame, and (3) a reasoning prompt specifying temporal or relational constraints. To enhance linguistic diversity and reduce annotation bias, question templates are generated using Qwen-2.5-VL-Instruct [56], conditioned on scene context, object attributes, and motion signals. All queries remain explicitly grounded in provided spatial annotations, ensuring no reliance on external commonsense inference. Additional details regarding dataset composition and train/test splits is included in Appendix §B.

5 Experiments

Evaluation Metrics. Let $B_t = \{x_t, y_t, w_t, h_t\}$ denote the bounding box at frame t , where (x_t, y_t) represents the center coordinates. For a trajectory of length T , B_t^{gt} and B_t^{pred} denote ground-truth and predicted boxes, respectively. We evaluate tracking quality using standard localization metrics (IoU, MOTP, CLE, NDE) along with our proposed Motion Consistency Precision (MCP), which explicitly measures temporal motion alignment. Detailed definitions are provided in Table 1. Unlike association-based metrics such as HOTA, MCP directly penalizes temporally implausible motion, making it particularly suitable

Table 1: Evaluation metrics for RMOT26.

Metric	Description
IoU	Spatial overlap between B_t^{pred} and B_t^{gt} per frame.
Center Distance	Euclidean distance between predicted and ground-truth centers (x_t, y_t) .
Direction Consistency (A_t)	Cosine similarity between predicted and ground-truth motion vectors Δ_t^{pred} and Δ_t^{gt} .
Speed Consistency (S_t)	Gaussian penalty on motion magnitude difference $\ \Delta_t^{pred}\ $ and $\ \Delta_t^{gt}\ $.
MCP	$MCP = \frac{1}{T-1} \sum_{t=2}^T A_t \cdot S_t.$

Table 2: Main results on the RMOT26 benchmark. Higher is better for MCP and MOTP, while lower is better for CLE and NDE.

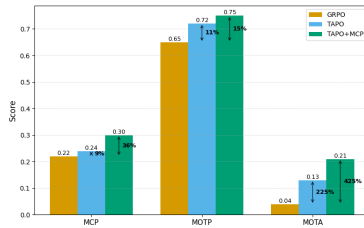
Model Name	Params	MCP↑	MOTP↑	CLE (px)↓	NDE↓
Open-Source Models					
Qwen2.5-VL-Instruct [56]	7B	0.24	0.48	289.2	2.07
Qwen3-VL-Instruct [57]	8B	<u>0.25</u>	0.64	96.0	0.97
Gemma 3 [55]	27B	0.24	0.56	<u>58.4</u>	0.88
Gemma 3 [55]	12B	0.18	<u>0.73</u>	172.9	0.95
Llama 3.2 Vision-Instruct [21]	11B	0.19	0.15	552.1	2.67
DeepSeek [67]	16B	0.11	0.27	989.13	4.7
Mistral-3-Instruct [33]	8B	0.15	0.54	225.3	0.98
Reasoning Models					
VisionReasoner [35]	7B	0.23	0.24	428.9	2.24
VisionReasoner [35]	3B	0.21	0.44	416.58	2.32
Migician [31]	7B	<u>0.25</u>	0.22	658.39	3.28
InternVL [11]	8B	0.21	0.66	117.44	0.64
Closed-Source Models					
gpt-4o-mini [38]	-	0.20	0.57	130.48	0.67
gpt-5.2 [51]	-	<u>0.25</u>	0.61	94.2	<u>0.55</u>
QTrack (Ours)	3B	0.30	0.75	44.61	0.39

for reasoning-based tracking. A detailed analysis of the MCP metric is provided in Appendix §D.1

Implementation Details. All experiments are conducted on a single NVIDIA H100 GPU (100GB memory). Training follows the GRPO-based reinforcement learning scheme described in Sec. 3.1. We adopt VisionReasoner [35] as our primary baseline, which employs GRPO-based policy optimization (Sec. 3.1). In addition to standard accuracy and format rewards, we introduce the MCP reward (Sec. 3.4) to explicitly supervise motion consistency. Furthermore, we integrate TAPO into the GRPO objective to enforce temporal sensitivity. Additional details regarding hyperparameters is written in Appendix §D.

Model (3B)	MCP↑	MOTP↑	NDE↓
VisionReasoner	0.21	0.44	2.32
GRPO	0.22	0.65	0.96
MCP-Reward	<u>0.25</u>	0.61	1.06
TAPO	0.24	<u>0.72</u>	<u>0.82</u>
QTrack (Ours)	0.30	0.75	0.39

(a) Component-wise



(b) GRPO vs TAPO comparison.

Fig. 4: Ablation analysis of QTrack components. TAPO significantly improves motion consistency and localization stability over GRPO.

(a) MOT17 Dataset

Model	MOTA	MOTP	HOTA	MCP
MOTR	0.61	0.81	0.22	<u>0.44</u>
BoostTrack++	0.63	0.76	0.38	0.44
TrackTrack	0.75	0.50	0.23	0.29
VisionReasoner	0.64	<u>0.86</u>	<u>0.60</u>	0.21
QTrack	<u>0.69</u>	0.87	0.69	0.26

(b) DanceTrack Dataset

Model	MOTA	MOTP	HOTA	MCP
MOTR	0.42	0.70	0.35	0.51
MOTRv2	0.49	0.73	0.37	<u>0.52</u>
TrackTrack	0.36	0.73	0.40	0.55
VisionReasoner	<u>0.59</u>	<u>0.85</u>	<u>0.61</u>	0.26
QTrack	0.63	0.83	0.66	0.35

Table 3: Comparison with traditional MOT methods. QTrack improves HOTA and MOTP while maintaining competitive MOTA.

5.1 Main Results on RMOT26

Table 2 presents comparisons across open-source, closed-source, and reasoning models. **Scaling alone does not ensure temporal reasoning.** We observe that increasing model size does not guarantee improved motion consistency. For instance, Gemma-3 (27B) achieves an MCP of 0.24, while Qwen-3-VL (8B) achieves 0.25, despite a significant parameter gap. This demonstrates that temporal consistency is not purely a scaling property but requires explicit motion supervision. **QTrack achieves the best overall performance.** QTrack (3B) achieves the highest MCP (0.30), highest MOTP (0.75), lowest CLE (44.61), and lowest NDE (0.39), outperforming all baselines. Notably, improvements are consistent across both spatial precision and temporal stability metrics, validating the effectiveness of structured rewards and TAPO regularization. Closed-source models are evaluated using identical prompts and deterministic decoding settings. We used a default temperature of 1.0 and default Top-p of 1.0.

5.2 Ablation Studies

Component Wise Results Fig 4(a) analyzes the contribution of each component. *GRPO improves spatial alignment but not motion stability.* While GRPO significantly improves MOTP (0.65), MCP remains limited (0.22), indicating insufficient temporal reasoning. *MCP reward improves motion consistency.* Introducing the MCP reward increases MCP to 0.25, confirming that explicit motion

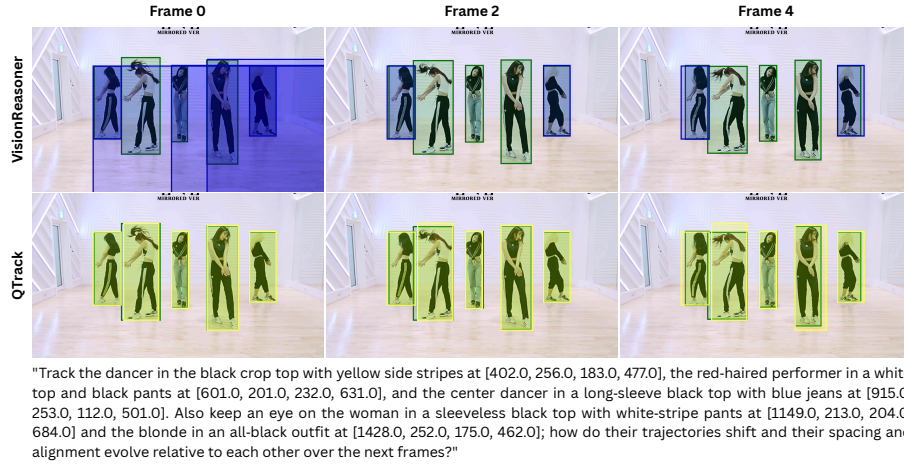


Fig. 5: In this figure, Visionreasoner is not able to detect and track all the objects in the frames, but QTrack is able to detect and track all objects in all frames.

supervision is essential for trajectory coherence. *TAPO enhances temporal robustness.* Integrating TAPO further improves MOTP (0.72) and reduces NDE (0.82), demonstrating reduced identity drift and improved motion sensitivity. *Full QTrack yields complementary gains.* The complete framework (GRPO + MCP + TAPO) achieves the best performance across all metrics. This confirms that spatial grounding, motion supervision, and temporal perception regularization are complementary and jointly necessary for reasoning-aware tracking.

GRPO vs TAPO. As illustrated in Fig. 4(b), GRPO improves reasoning quality but often produces temporally invariant trajectories. TAPO explicitly enforces motion sensitivity, resulting in smoother trajectories, reduced drift, and significantly higher MCP.

Comparison with Traditional MOT Methods. Tables 3a and 3b compare QTrack against recent MOT methods on MOT17 [40] and DanceTrack [52]. On MOT17, QTrack achieves the best MOTP (0.87) and HOTA (0.69), while maintaining competitive MOTA (0.69). On DanceTrack, QTrack achieves the best MOTA (0.63) and HOTA (0.66). Since **QTrack** is not a traditional MOT model, it is important to note that this comparison is conducted on short query-specific segments derived from the benchmark sequences rather than entire videos. Traditional MOT methods track all objects indiscriminately, whereas **QTrack** selectively tracks query-specified targets. Despite this stricter constraint, **QTrack** remains competitive or superior on standard tracking metrics, demonstrating that reasoning-aware tracking does not compromise trajectory quality. Details of the evaluation protocol used for traditional MOT models are provided in Appendix §E.

Qualitative Analysis. Figure 5 presents qualitative comparisons. VisionReasoner fails to consistently localize all targets across frames, particularly under

occlusion and appearance ambiguity. In contrast, QTrack maintains stable identities and coherent motion trajectories, demonstrating improved multi-object reasoning and temporal robustness. Detailed qualitative analysis is shown in Appendix §G.

6 Conclusion

We introduced **QTrack**, a query-driven tracking paradigm that reformulates multi-object tracking as a reasoning-aware, language-conditioned problem. To this end, we curated the **RMOT26** benchmark for evaluating fine-grained spatiotemporal reasoning under explicit query grounding. In addition, we further proposed a reinforcement learning-based framework with structured rewards and Temporal Perception-Aware Policy Optimization (TAPO), explicitly enforcing motion consistency and identity persistence. **QTrack** achieves state-of-the-art performance on **RMOT26**, improving MCP by **+5% absolute** over the strongest baseline (0.30 vs. 0.25) and reducing NDE by more than **50%** (0.39 vs. 0.82 in ablations). On traditional MOT benchmarks, QTrack remains competitive despite selectively tracking query-specified objects, achieving the best HOTA on MOT17 (+9% relative over prior reasoning models) and the best MOTA and HOTA on DanceTrack, demonstrating that reasoning-aware tracking does not sacrifice trajectory quality. These results highlight that explicit motion supervision and temporal perception optimization are more critical than model scaling alone for robust spatiotemporal reasoning.

Bibliography

- [1] Abdar, M., Kollati, M., Kuraparthi, S., Pourpanah, F., McDuff, D., Ghavamzadeh, M., Yan, S., Mohamed, A., Khosravi, A., Cambria, E., et al.: A review of deep learning for video captioning. *IEEE Transactions on Pattern Analysis and Machine Intelligence* (2024) [5](#)
- [2] Abeysinghe, C., Reid, C., Rezatofighi, H., Meyer, B.: Tracking different ant species: an unsupervised domain adaptation framework and a dataset for multi-object tracking. *arXiv preprint arXiv:2301.10559* (2023) [10](#)
- [3] Al-Tahan, H., Garrido, Q., Balestrieri, R., Bouchacourt, D., Hazirbas, C., Ibrahim, M.: Unibench: Visual reasoning requires rethinking vision-language beyond scaling. *Advances in Neural Information Processing Systems* **37**, 82411–82437 (2024) [3](#)
- [4] Alayrac, J.B., Donahue, J., Luc, P., et al.: Flamingo: A visual language model for few-shot learning. *NeurIPS* (2022) [5](#)
- [5] Andriluka, M., Roth, S., Schiele, B.: People-tracking-by-detection and people-detection-by-tracking. In: 2008 IEEE Conference on computer vision and pattern recognition. pp. 1–8. *IEEE* (2008) [4](#)
- [6] Ashraf, T., Bin Afzal Mir, F., Gillani, I.A.: Transfed: A way to epitomize focal modulation using transformer-based federated learning. In: *Proceedings of the IEEE/CVF Winter Conference on Applications of Computer Vision*. pp. 554–563 (2024) [4](#)
- [7] Bernardin, K., Stiefelhagen, R.: Evaluating multiple object tracking performance: the clear mot metrics. *EURASIP Journal on Image and Video Processing* **2008**(1), 246309 (2008) [1](#)
- [8] Bewley, A., Ge, Z., Ott, L., Ramos, F., Upcroft, B.: Simple online and realtime tracking. In: *ICIP* (2016) [4](#)
- [9] Bochinski, E., Eiselein, V., Sikora, T.: High-speed tracking-by-detection without using image information. In: 2017 14th IEEE international conference on advanced video and signal based surveillance (AVSS). pp. 1–6. *IEEE* (2017) [4](#)
- [10] Breitenstein, M.D., Reichlin, F., Leibe, B., Koller-Meier, E., Van Gool, L.: Robust tracking-by-detection using a detector confidence particle filter. In: 2009 IEEE 12th International Conference on Computer Vision. pp. 1515–1522. *IEEE* (2009) [4](#)
- [11] Chen, Z., Wu, J., Wang, W., Su, W., Chen, G., Xing, S., Zhong, M., Zhang, Q., Zhu, X., Lu, L., et al.: Internvl: Scaling up vision foundation models and aligning for generic visual-linguistic tasks. In: *Proceedings of the IEEE/CVF conference on computer vision and pattern recognition*. pp. 24185–24198 (2024) [12](#)
- [12] Ciaparrone, G., Sánchez, F.L., Tabik, S., Troiano, L., Tagliaferri, R., Herrera, F.: Deep learning in video multi-object tracking: A survey. *Neurocomputing* **381**, 61–88 (2020) [2](#)

- [13] Cui, Y., Zeng, C., Zhao, X., Yang, Y., Wu, G., Wang, L.: Sportsmot: A large multi-object tracking dataset in multiple sports scenes. arXiv preprint arXiv:2304.05170 (2023) [4](#), [10](#)
- [14] Dave, A., Khurana, T., Tokmakov, P., Schmid, C., Ramanan, D.: Tao: A large-scale benchmark for tracking any object. In: European conference on computer vision. pp. 436–454. Springer (2020) [4](#), [10](#)
- [15] Dendorfer, P., Osep, A., Milan, A., Schindler, K., Cremers, D., Reid, I., Roth, S., Leal-Taixé, L.: Motchallenge: A benchmark for single-camera multiple target tracking: P. dendorfer et al. International Journal of Computer Vision **129**(4), 845–881 (2021) [4](#)
- [16] Dendorfer, P., Rezatofghi, H., Milan, A., Shi, J., Cremers, D., Reid, I., Roth, S., Schindler, K., Leal-Taixé, L.: Mot20: A benchmark for multi object tracking in crowded scenes. arXiv preprint arXiv:2003.09003 (2020) [4](#), [10](#)
- [17] Ding, S., Wu, S., Zhao, X., Zang, Y., Duan, H., Dong, X., Zhang, P., Cao, Y., Lin, D., Wang, J.: Mm-ifengine: Towards multimodal instruction following. In: Proceedings of the IEEE/CVF International Conference on Computer Vision. pp. 1099–1109 (2025) [3](#)
- [18] Ding, Y., Chen, Z., Liu, Z., Wang, L.: Mevis: A benchmark for multi-event video segmentation with natural language expressions. In: ICCV (2023) [4](#)
- [19] Ferryman, J., Shahrokhni, A.: Pets2009: Dataset and challenge. In: 2009 Twelfth IEEE International Workshop on Performance Evaluation of Tracking and Surveillance. pp. 1–6 (2009). <https://doi.org/10.1109/PETS-WINTER.2009.5399556> [4](#), [10](#)
- [20] Gavriilyuk, K., Ghodrati, A., Li, X., Snoek, C.: Actor and action video segmentation from a sentence. In: CVPR (2018) [4](#)
- [21] Grattafiori, A., Dubey, A., Jauhri, A., Pandey, A., Kadian, A., Al-Dahle, A., Letman, A., Mathur, A., Schelten, A., Vaughan, A., et al.: The llama 3 herd of models. arXiv preprint arXiv:2407.21783 (2024) [12](#)
- [22] Grunde-McLaughlin, L., He, J., Abbeel, P., Darrell, T.: Agqa: A benchmark for compositional spatio-temporal reasoning. In: CVPR (2021) [5](#)
- [23] Guo, D., Yang, D., Zhang, H., Song, J., Wang, P., Zhu, Q., Xu, R., Zhang, R., Ma, S., Bi, X., et al.: Deepseek-r1: Incentivizing reasoning capability in llms via reinforcement learning. arXiv preprint arXiv:2501.12948 (2025) [5](#)
- [24] He, L., Zhou, Q., Li, X., Niu, L., Cheng, G., Li, X., Liu, W., Tong, Y., Ma, L., Zhang, L.: Imagenet vid dataset (dec 2024). <https://doi.org/10.57702/58xou3kx>, <https://service.tib.eu/ldmservice/dataset/imagenet-vid-dataset> [4](#)
- [25] HOU, Y.: Uavdt (Dec 2024). <https://doi.org/10.5281/zenodo.14575517>, <https://doi.org/10.5281/zenodo.14575517> [4](#)
- [26] Iashin, V., Rahtu, E.: Multi-modal dense video captioning. In: Proceedings of the IEEE/CVF conference on computer vision and pattern recognition workshops. pp. 958–959 (2020) [5](#)
- [27] Jang, Y., Song, Y., Yu, Y., Kim, Y., Kim, G.: Tgif-qa: Toward spatio-temporal reasoning in visual question answering. In: CVPR (2017) [5](#)
- [28] Kalake, L., Wan, W., Hou, L.: Analysis based on recent deep learning approaches applied in real-time multi-object tracking: a review. IEEE Access **9**, 32650–32671 (2021) [1](#)

- [29] Leal-Taixé, L., Milan, A., Reid, I., Roth, S., Schindler, K.: Motchallenge 2015: Towards a benchmark for multi-target tracking. arXiv preprint arXiv:1504.01942 (2015) [4](#), [10](#)
- [30] Li, Y., Huang, C., Li, X., Yang, X., Hua, G., Zhang, H.: Tracking by natural language specification. In: CVPR (2017) [4](#)
- [31] Li, Y., Huang, H., Chen, C., Huang, K., Huang, C., Guo, et al.: Migician: Revealing the magic of free-form multi-image grounding in multimodal large language models. In: Findings of the Association for Computational Linguistics (ACL 2025). pp. 9845–9867 (2025) [12](#)
- [32] Li, Y., Wang, N., Zhou, W., Li, H.: Lamot: Language-based multi-object tracking. In: CVPR (2024) [4](#), [7](#)
- [33] Liu, A.H., Khandelwal, K., Subramanian, S., Jouault, V., Rastogi, A., Sadé, A., Jeffares, A., Jiang, A., Cahill, A., Gavaudan, A., et al.: Ministral 3. arXiv preprint arXiv:2601.08584 (2026) [12](#)
- [34] Liu, Y., Peng, B., Zhong, Z., Yue, Z., Lu, F., Yu, B., Jia, J.: Seg-zero: Reasoning-chain guided segmentation via cognitive reinforcement. arXiv preprint arXiv:2503.06520 (2025) [5](#)
- [35] Liu, Y., Qu, T., Zhong, Z., Peng, B., Liu, S., Yu, B., Jia, J.: Visionreasoner: Unified visual perception and reasoning via reinforcement learning. arXiv preprint arXiv:2505.12081 (2025) [12](#), [36](#)
- [36] Liu, Z., Sun, Z., Zang, Y., Dong, X., Cao, Y., Duan, H., Lin, D., Wang, J.: Visual-rft: Visual reinforcement fine-tuning. In: Proceedings of the IEEE/CVF International Conference on Computer Vision. pp. 2034–2044 (2025) [5](#)
- [37] Luo, W., Xing, J., Milan, A., Zhang, X., Liu, W., Kim, T.K.: Multiple object tracking: A literature review. *Artificial intelligence* **293**, 103448 (2021) [1](#)
- [38] Mao, J., Huang, J., Toshev, A., Camburu, O., Yuille, A.L., Murphy, K.: Generation and comprehension of unambiguous object descriptions. In: Proceedings of the IEEE conference on computer vision and pattern recognition. pp. 11–20 (2016) [12](#)
- [39] Meimetus, D., Daramouskas, I., Perikos, I., Hatzilygeroudis, I.: Real-time multiple object tracking using deep learning methods. *Neural Computing and Applications* **35**(1), 89–118 (2023) [2](#)
- [40] Milan, A., Leal-Taixé, L., Reid, I., Roth, S., Schindler, K.: Mot16: A benchmark for multi-object tracking. arXiv preprint arXiv:1603.00831 (2016) [4](#), [10](#), [14](#), [36](#)
- [41] Niu, T.Z., Chen, Z.D., Luo, X., Zhang, P.F., Huang, Z., Xu, X.S.: Video captioning by learning from global sentence and looking ahead. *ACM Transactions on Multimedia Computing, Communications and Applications* **19**(5s), 1–20 (2023) [5](#)
- [42] Ouyang, L., Wu, J., Jiang, X., Almeida, D., Wainwright, C., Mishkin, P., Zhang, C., Agarwal, S., Slama, K., Ray, A., et al.: Training language models to follow instructions with human feedback. *Advances in neural information processing systems* **35**, 27730–27744 (2022) [5](#)
- [43] Pal, S.K., Pramanik, A., Maiti, J., Mitra, P.: Deep learning in multi-object detection and tracking: state of the art. *Applied Intelligence* **51**(9), 6400–6429 (2021) [2](#), [4](#)

- [44] Radford, A., Kim, J.W., Hallacy, C., Ramesh, A., Goh, G., Agarwal, S., et al.: Learning transferable visual models from natural language supervision. In: ICML (2021) 5
- [45] Rafailov, R., Sharma, A., Mitchell, E., Manning, C.D., Ermon, S., Finn, C.: Direct preference optimization: Your language model is secretly a reward model. *Advances in neural information processing systems* **36**, 53728–53741 (2023) 5
- [46] Samleti, S., Mishra, A., Jhahhria, A., Rai, S.K., Malik, G.: Real time video captioning using deep learning. *INTERNATIONAL JOURNAL OF ENGINEERING RESEARCH and TECHNOLOGY (IJERT)* **10**(12) (2021) 5
- [47] Schulman, J., Wolski, F., Dhariwal, P., Radford, A., Klimov, O.: Proximal policy optimization algorithms. *arXiv preprint arXiv:1707.06347* (2017) 5
- [48] Shao, Z., Wang, P., Zhu, Q., Xu, R., Song, J., Bi, X., Zhang, H., Zhang, M., Li, Y., Wu, Y., et al.: Deepseekmath: Pushing the limits of mathematical reasoning in open language models. *arXiv preprint arXiv:2402.03300* (2024) 5
- [49] Shim, K., Ko, K., Yang, Y., Kim, C.: Focusing on tracks for online multi-object tracking. In: *Proceedings of the IEEE/CVF Conference on Computer Vision and Pattern Recognition (CVPR)*. pp. 11687–11696 (June 2025) 1
- [50] Shingare, S., Haribhakta, Y., Rajmane, D.: Video captioning using deep learning and nlp to detect suspicious activities. In: *2022 International Conference on Signal and Information Processing (IConSIP)*. pp. 1–5. *IEEE* (2022) 5
- [51] Singh, A., Fry, A., Perelman, A., Tart, A., Ganesh, A., El-Kishky, A., McLaughlin, A., Low, A., Ostrow, A., Ananthram, A., et al.: Openai gpt-5 system card. *arXiv preprint arXiv:2601.03267* (2025) 12
- [52] Sun, P., Cao, J., Jiang, Y., Yuan, Z., Bai, S., Kitani, K., Luo, P.: Dance-track: Multi-object tracking in uniform appearance and diverse motion. In: *Proceedings of the IEEE/CVF conference on computer vision and pattern recognition*. pp. 20993–21002 (2022) 4, 10, 14, 36
- [53] Sun, Z., Chen, J., Chao, L., Ruan, W., Mukherjee, M.: A survey of multiple pedestrian tracking based on tracking-by-detection framework. *IEEE Transactions on Circuits and Systems for Video Technology* **31**(5), 1819–1833 (2020) 4
- [54] Tan, H., Ji, Y., Hao, X., Chen, X., Wang, P., Wang, Z., Zhang, S.: Reason-rft: Reinforcement fine-tuning for visual reasoning of vision language models (2025), <https://api.semanticscholar.org/CorpusID:281842907> 3
- [55] Team, G., et al.: Gemma 3 technical report (2025), <https://arxiv.org/abs/2503.19786> 12, 36
- [56] Team, Q.: Qwen2.5-vl (January 2025), <https://qwenlm.github.io/blog/qwen2.5-vl/> 11, 12, 23, 36
- [57] Team, Q.: Qwen3 technical report (2025), <https://arxiv.org/abs/2505.09388> 12
- [58] Tomasi, C., Kanade, T.: Detection and tracking of point. *Int J Comput Vis* **9**(137-154), 3 (1991) 4

- [59] Tong, S., Brown, E., Wu, P., Woo, S., Middepogu, M., Akula, S.C., Yang, J., Yang, S., Iyer, A., Pan, X., Wang, A., Fergus, R., LeCun, Y., Xie, S.: Cambrian-1: A fully open, vision-centric exploration of multimodal llms. ArXiv [abs/2406.16860](https://arxiv.org/abs/2406.16860) (2024), <https://api.semanticscholar.org/CorpusID:270703300> **3**
- [60] Voigtlaender, P., Krause, M., Ošep, A., Luiten, J., Sekar, B.B.G., Geiger, A., Leibe, B.: MOTs: Multi-object tracking and segmentation. In: CVPR (2019) **4**
- [61] Wang, B., Ma, L., Zhang, W., Liu, W.: Reconstruction network for video captioning. In: Proceedings of the IEEE conference on computer vision and pattern recognition. pp. 7622–7631 (2018) **5**
- [62] Wang, N., Zhou, W., Li, Y., Tan, Z., Li, J.: Tnl2k: Benchmarking tracking by natural language specification. In: CVPR (2021) **4**
- [63] Wang, Z., Guo, X., Stoica, S., Xu, H., Wang, H., Ha, H., Chen, X., Chen, Y., Yan, M., Huang, F., et al.: Perception-aware policy optimization for multimodal reasoning. arXiv preprint arXiv:2507.06448 (2025) **5**
- [64] Wei, Y., Zhao, L., Sun, J., Lin, K., Yin, J., Hu, J., Zhang, Y., Yu, E., Lv, H., Weng, Z., Wang, J., Han, C., Peng, Y., Han, Q., Ge, Z., Zhang, X.T., Jiang, D., Patel, V.M.: Open vision reasoner: Transferring linguistic cognitive behavior for visual reasoning. ArXiv [abs/2507.05255](https://arxiv.org/abs/2507.05255) (2025), <https://api.semanticscholar.org/CorpusID:280068664> **3**
- [65] Wojke, N., Bewley, A., Paulus, D.: Simple online and realtime tracking with a deep association metric. In: ICIP (2017) **4, 7**
- [66] Wu, T., Zeng, L., Zhang, L.: Language as queries for referring video object segmentation. In: CVPR (2022) **4**
- [67] Wu, Z., Chen, X., Pan, Z., Liu, X., Liu, W., Dai, D., Gao, H., Ma, Y., Wu, C., Wang, B., Xie, Z., Wu, Y., Hu, K., Wang, J., Sun, Y., Li, Y., Piao, Y., Guan, K., Liu, A., Xie, X., You, Y., Dong, K., Yu, X., Zhang, H., Zhao, L., Wang, Y., Ruan, C.: Deepseek-vl2: Mixture-of-experts vision-language models for advanced multimodal understanding (2024), <https://arxiv.org/abs/2412.10302> **12**
- [68] Xiao, J., Shang, X., Yao, T., Mei, T.: Next-qa: Next phase of question-answering for temporal and causal reasoning in video. In: CVPR (2021) **5**
- [69] Xu, K., Sun, T., Jiang, X.: Video anomaly detection and localization based on an adaptive intra-frame classification network. IEEE Transactions on Multimedia **22**(2), 394–406 (2019) **7**
- [70] Yan, S., Xiong, X., Nagrani, A., Arnab, A., Wang, Z., Ge, W., Ross, D., Schmid, C.: Unloc: A unified framework for video localization tasks. In: Proceedings of the IEEE/CVF International Conference on Computer Vision. pp. 13623–13633 (2023) **7**
- [71] Yu, F., Xian, W., Chen, Y., Liu, F., Liao, M., Madhavan, V., Darrell, T., et al.: Bdd100k: A diverse driving video database with scalable annotation tooling. arXiv preprint arXiv:1805.04687 **2**(5), 6 (2018) **4**
- [72] Zhang, H., Li, H., Li, F., Ren, T., Zou, X., Liu, S., Huang, S., Gao, J., Leizhang, Li, C., et al.: Llava-grounding: Grounded visual chat with large

- multimodal models. In: European Conference on Computer Vision. pp. 19–35. Springer (2024) [3](#)
- [73] Zhang, L., Gao, J., Xiao, Z., Fan, H.: Animaltrack: A benchmark for multi-animal tracking in the wild. *International Journal of Computer Vision* **131**(2), 496–513 (2023) [4](#)
- [74] Zhang, Y., Wang, C., Wang, X., Zeng, W., Liu, W.: Fairmot: On the fairness of detection and re-identification in multiple object tracking. *International journal of computer vision* **129**(11), 3069–3087 (2021) [4](#), [7](#)
- [75] Zheng, Y., Lu, J., Wang, S., Feng, Z., Kuang, D., Xiong, Y.: Easyr1: An efficient, scalable, multi-modality rl training framework. <https://github.com/hiyouga/EasyR1> (2025) [5](#)
- [76] Zhou, J., Lu, T., Mishra, S., Brahma, S., Basu, S., Luan, Y., Zhou, D., Hou, L.: Instruction-following evaluation for large language models. *ArXiv abs/2311.07911* (2023), <https://api.semanticscholar.org/CorpusID:265157752> [3](#)
- [77] Zhu, P., Wen, L., Du, D., Bian, X., Fan, H., Hu, Q., Ling, H.: Detection and tracking meet drones challenge. *IEEE Transactions on Pattern Analysis and Machine Intelligence* **44**(11), 7380–7399 (2021) [4](#)
- [78] Zhu, P., Wen, L., Du, D., Bian, X., Fan, H., Hu, Q., Ling, H.: Detection and tracking meet drones challenge. *IEEE transactions on pattern analysis and machine intelligence* **44**(11), 7380–7399 (2021) [4](#)

Appendix for QTrack: Query-Driven Reasoning for Multi-modal MOT

Appendix Section	Description
Section A	RMOT26 Data Card
Section B	RMOT26 Dataset Statistics
Section C	Detailed Reward Function Formulation
Section D	Metrics and Implementation Details
Section E	Evaluation Protocol for Traditional MOT Comparison
Section F	Comparison with Fine-Tuned Models
Section G	Additional Qualitative Results
Section H	Failure Cases
Section I	Prompt Templates for Baseline Models

A Datacard for RMOT26

A.1 Motivation

- **For what purpose was the dataset created?**
The RMOT26 dataset is designed to evaluate *query-driven multi-object tracking*, where models track only objects specified by a natural language query rather than all objects in a scene. Each task requires identifying the correct object(s) in a reference frame and maintaining consistent trajectories across subsequent frames. The dataset evaluates language-conditioned spatiotemporal reasoning, including query understanding, spatial grounding, temporal identity consistency, and robustness under challenging conditions such as occlusion or object interactions.
- **Who created the dataset?**
The dataset was created by the authors of this paper.
- **Who funded the creation of the dataset?**
Funding information will be disclosed after the anonymous review process.

A.2 Composition

- **What do the individual instances represent?**
Each instance represents a query-conditioned tracking task consisting of a reference frame with annotated bounding boxes, a sequence of subsequent frames, a natural language query describing the target object(s), and ground-truth trajectories.

- **How many instances are there?**
The dataset contains 1000 instances: 900 single-object tracking tasks and 100 multi-object tracking tasks. Among the single-object tasks, 20 queries specifically focus on occlusion scenarios.
- **Is the dataset a complete set or a sample?**
The dataset is a curated collection of tracking scenarios rather than an exhaustive set.
- **What data does each instance contain?**
Each instance includes a reference frame, subsequent video frames, a natural language query, and ground-truth bounding box trajectories with object IDs.
- **Is there a label associated with each instance?**
Yes. Ground-truth bounding boxes and object IDs define the target trajectories.
- **Is any information missing from instances?**
No.
- **Are there recommended data splits?**
Yes. The dataset provides predefined training and test splits described in Section B.
- **Are there errors or noise in the dataset?**
The dataset is generated using a semi-automated pipeline and verified by humans. Minor annotation noise may occur due to human error.
- **Does the dataset rely on external resources?**
Yes. The video sequences are derived from existing multi-object tracking datasets.
- **Does the dataset contain confidential data?**
No.
- **Does the dataset contain potentially offensive content?**
No.

A.3 Collection Process

- **How was the data acquired?**
Language queries and reasoning steps were generated using Qwen2.5-VL-Instruct [56] and subsequently reviewed and refined by human annotators. The visual data was collected from publicly available datasets.
- **What methods were used to generate and curate the data?**
A semi-automated pipeline was used. Queries, reasoning steps, and candidate outputs were first generated by Qwen2.5-VL-Instruct and then manually verified for correctness and clarity.
- **Who was involved in the data collection process?**
Researchers and student annotators.
- **Over what timeframe was the data collected?**
The dataset was created between 2025 and 2026.
- **Were ethical considerations taken into account?**
Yes. All visual data comes from datasets released for academic research. Removal requests from original dataset authors will be honored.

A.4 Preprocessing/Cleaning/Labeling

- **Was preprocessing or annotation performed?**
Yes. Automatically generated queries and reasoning outputs were manually reviewed and corrected before inclusion.
- **Was the raw data saved?**
No separate raw data is stored. The dataset contains curated subsets of images and videos from existing datasets along with generated annotations.

A.5 Uses

- **Has the dataset already been used for tasks?**
Yes. It is used in this paper to evaluate query-driven multi-object tracking.
- **Is there a repository listing papers using the dataset?**
No.
- **What other tasks could this dataset support?**
The dataset can support research in vision-language reasoning, multimodal grounding, and agent-based visual decision-making.
- **Could the dataset composition impact future uses?**
No known limitations are expected.
- **Are there potential negative social impacts?**
No direct negative social impacts are anticipated.

A.6 Distribution

- **Will the dataset be distributed externally?**
Yes.
- **How will the dataset be distributed?**
The dataset will be released through a public GitHub repository.
- **Under what license will it be released?**
The dataset will be released under the Apache License.
- **Are there any third-party restrictions?**
No.

A.7 Maintenance

- **Who will maintain the dataset?**
The authors of this paper.
- **How can the maintainers be contacted?**
Contact details are provided in the paper.
- **Will the dataset be updated?**
Yes. Updates and corrections will be made through the GitHub repository.
- **Can others contribute to the dataset?**
Yes. Contributions and suggestions can be proposed through GitHub or by contacting the authors.

Scenario	Reference Frame	Query	Frame 0	Frame 1	Frame 2	Frame 3
Crowded Scene		"Observe how the person wearing a black hoodie and jeans, carrying a bag, moves along the sidewalk as he walk away from the camera."				
Partial Occlusion		"Observe how the person wearing a light blue shirt and jeans, occluded by a person wearing a yellow shirt and black jeans, keeping an eye on his trajectory as he walks past the LG OLED TV advertisement."				
Complete Occlusion		"Track the person wearing black colored clother, fully occluded by a person with blue shirt and white jeans moves through the mall."				
Similar Appearance		"Track the dancer in a black tee with a white addidas logo, the blonde wearing a white crop top, the woman in the black crop top, and the red-haired performer in a black outfit with a white band across the chest. Observe..."				
Reference Target Tracking Challenges: Crowded Partial Occlusion Complete Occlusion Similar Appearance		RMOT26 Dataset Examples				
		Each row showcases a challenging scenario: crowded scenes , partial occlusion , complete occlusion and similar appearance distractors . The sequence includes a reference frame, query appearance and future frames (0 to 3).				

Fig. 6: Overview of the RMOT26 dataset components. The dataset contains four types of query scenarios: (1) crowded scenes, (2) partial occlusion, (3) complete occlusion, and (4) similar-appearance distractors. These cases require models to perform robust language-guided tracking under challenging visual conditions.

B RMOT26 Dataset Statistics

The RMOT26 dataset is constructed by curating video sequences from seven existing multi-object tracking (MOT) benchmarks. To ensure fair evaluation and avoid identity leakage between training and testing sets, all splits are performed at the sequence level rather than the frame level. Figure 6 illustrates the key components and challenging scenarios represented in the dataset. In particular, the dataset includes four types of query conditions: (1) crowded scenes, (2) partial occlusion, (3) complete occlusion, and (4) similar-appearance distractors. These scenarios require models to perform both spatial grounding and temporal reasoning when tracking objects specified by natural language queries.

B.1 Dataset Composition

Each instance in the dataset consists of a reference frame followed by a short future sequence of 5–6 frames. The dataset is constructed using sequences from multiple existing MOT benchmarks to ensure diversity in scene types, motion patterns, and tracking difficulty. Table 4 summarizes the dataset composition, showing the contribution of each source dataset to the training and test sets in terms of sequences and frames.

B.2 Train / Test Splits

The overall dataset statistics for the training and test splits are presented in Table 5. The training set contains 1,636 sequences and 6,678 frames, while the

Table 4: Composition of the RMOT26 dataset derived from existing MOT benchmarks.

Dataset	Train		Test	
	Sequences	Frames	Sequences	Frames
MOT17	253	1058	242	995
MOT16	122	535	66	284
MOT20	73	305	46	190
DanceTrack	962	3864	574	2275
SportsMOT	73	297	2	8
PETS	21	81	2	6
DAMUNT	132	538	68	250

test set includes 1,000 sequences and 4,008 frames. These splits ensure a balanced distribution of scenes and tracking conditions while preventing sequence overlap between the training and evaluation sets.

Table 5: Overall RMOT26 dataset statistics for training and test splits.

	Split	Sequences	Frames
Train	1636	6678	
Test	1000	4008	

C Detailed Reward Function Formulation

In the main paper (Section 3.4), we introduced a unified reward mechanism that combines structured reasoning supervision, spatial localization accuracy, and temporal motion consistency. In this appendix section, we provide additional implementation details for each reward component, including the reasoning format constraint and the structured output requirements used during training.

C.1 Thinking Format Reward

The *Thinking Format Reward* encourages the model to generate structured reasoning traces before producing bounding box predictions. Specifically, the output must follow a predefined structure consisting of two components: a reasoning section enclosed in `<think>` tags and a prediction section enclosed in `<answer>` tags. Below diagram illustrates the required response structure expected from the model.

Required Output Structure

```

<think>
  reasoning steps explaining how the target
  object is identified and tracked
</think>

<answer>
  bounding box predictions
</answer>

```

This structure encourages models to explicitly reason about the visual scene and the query before producing the tracking outputs. During training, the generated output is verified using a rule-based validator to ensure that the required tags are present and properly structured. Table 6 summarizes the reward assignment for different formatting conditions.

Table 6: Thinking format reward conditions.

Condition	Output Format	Reward
Correct tags	Valid reasoning and answer enclosed in <code><think></code> and <code><answer></code>	1.0
Missing tags	Output lacks either <code><think></code> or <code><answer></code> tags	0.0
Malformed tags	Incorrect or mismatched tag structure causing regex mismatch	0.0

C.2 Answer Format Reward

In addition to structured reasoning, the model must produce tracking predictions in a structured JSON format so that outputs can be reliably parsed and evaluated during training. Each prediction contains the frame index and the corresponding bounding box coordinates represented using the `[x1,y1,x2,y2]` format, where (x_1, y_1) and (x_2, y_2) denote the top-left and bottom-right corners of the bounding box, respectively.

Single Object Prediction Format

```

[
  {"frame": frame_id, "bbox": [x1, y1, x2, y2]},
  {"frame": frame_id, "bbox": [x1, y1, x2, y2]}
]

```

Multiple Object Prediction Format

```
[
  {"frame": frame_id, "object_id": 1, "bbox": [x1, y1, x2, y2]},
  {"frame": frame_id, "object_id": 2, "bbox": [x1, y1, x2, y2]},
  {"frame": frame_id, "object_id": 3, "bbox": [x1, y1, x2, y2]}
]
```

The model always outputs bounding boxes in the $[x_1, y_1, x_2, y_2]$ representation. However, the ground-truth annotations in the dataset are stored using the $[x, y, w, h]$ format, where (x, y) corresponds to the top-left corner of the bounding box and (w, h) denote its width and height.

To ensure consistency during reward computation, all ground-truth annotations are converted to the $[x_1, y_1, x_2, y_2]$ format prior to evaluation using the following transformation:

$$x_1 = x, \quad y_1 = y$$

$$x_2 = x + w, \quad y_2 = y + h$$

After this conversion, both predicted and ground-truth bounding boxes share the same coordinate representation. Consequently, all subsequent reward components, including IoU computation, geometric distance rewards, and temporal motion consistency, operate on bounding boxes represented in the $[x_1, y_1, x_2, y_2]$ format.

During evaluation, model outputs are first validated using a strict JSON parser. If strict parsing fails due to minor formatting issues, a regex-based fallback parser is applied to extract the relevant fields such as `frame`, `bbox`, and optional `object_id`. This fallback mechanism improves robustness by allowing slightly malformed outputs to be recovered while preserving the required bounding box coordinate structure.

C.3 IoU-Based Spatial Reward

Spatial localization quality is evaluated using the intersection-over-union (IoU) between predicted and ground-truth bounding boxes. Let $B^{pred} = \{b_i^{pred}\}_{i=1}^M$ denote the set of predicted bounding boxes and $B^{gt} = \{b_j^{gt}\}_{j=1}^N$ denote the corresponding ground-truth boxes. Each bounding box is represented using the corner-coordinate format

$$b = (x_1, y_1, x_2, y_2),$$

where (x_1, y_1) and (x_2, y_2) denote the top-left and bottom-right corners of the bounding box.

For a predicted box b_i^{pred} and a ground-truth box b_j^{gt} , the IoU score is defined as

$$IoU(b_i^{pred}, b_j^{gt}) = \frac{\text{Area}(b_i^{pred} \cap b_j^{gt})}{\text{Area}(b_i^{pred} \cup b_j^{gt})}.$$

A binary IoU reward is assigned using a threshold $\tau_{IoU} = 0.5$:

$$r_{IoU}(i, j) = \begin{cases} 1 & \text{if } IoU(b_i^{pred}, b_j^{gt}) > 0.5, \\ 0 & \text{otherwise.} \end{cases}$$

This reward provides strong supervision when the predicted box sufficiently overlaps with the ground-truth object. However, IoU alone can produce sparse reward signals when predictions are close to the ground truth but do not yet meet the overlap threshold. To provide additional gradient signals during training, we incorporate two auxiliary geometric rewards: a bounding-box L1 reward and a point localization reward.

Bounding Box L1 Reward To capture geometric proximity between predicted and ground-truth boxes, we compute the mean L1 distance between their coordinates:

$$d_{L1}(i, j) = \frac{1}{4} \sum_{k=1}^4 |b_{i,k}^{pred} - b_{j,k}^{gt}|.$$

A binary reward is assigned using threshold $\tau_{L1} = 10$:

$$r_{L1}(i, j) = \begin{cases} 1 & \text{if } d_{L1}(i, j) < 10, \\ 0 & \text{otherwise.} \end{cases}$$

This reward provides partial credit when predicted boxes are geometrically close to the ground truth even if the IoU threshold is not satisfied.

Point Localization Reward To further encourage accurate localization, we evaluate the distance between predicted and ground-truth keypoints. Let $p_i^{pred} = (x_i, y_i)$ and $p_j^{gt} = (x_j, y_j)$ denote the predicted and ground-truth keypoints. Their Euclidean distance is

$$d_{point}(i, j) = \sqrt{(x_i - x_j)^2 + (y_i - y_j)^2}.$$

A point reward is assigned if the predicted point is spatially close to the ground truth and lies inside the predicted bounding box:

$$r_{point}(i, j) = \begin{cases} 1 & \text{if } d_{point}(i, j) < 30 \wedge p_i^{pred} \in b_i^{pred}, \\ 0 & \text{otherwise.} \end{cases}$$

The point-in-box constraint is defined as

$$x_1 \leq x_i \leq x_2 \quad \text{and} \quad y_1 \leq y_i \leq y_2.$$

This additional constraint prevents trivial solutions where points are predicted near the ground truth but outside the bounding box.

Reward Aggregation and Instance Matching For each predicted-ground-truth pair (i, j) , the individual reward components are combined to form a unified reward score

$$R_{ij} = r_{IoU}(i, j) + r_{L1}(i, j) + r_{point}(i, j).$$

All pairwise rewards are computed to construct a reward matrix of size $M \times N$. To obtain the optimal alignment between predicted and ground-truth instances, we convert the reward matrix into a cost matrix

$$C_{ij} = 3 - R_{ij}.$$

The Hungarian algorithm is then applied to solve the bipartite matching problem

$$\mathcal{M}^* = \arg \min_{\mathcal{M}} \sum_{(i,j) \in \mathcal{M}} C_{ij}.$$

Finally, the normalized spatial reward is computed as

$$R_{final} = \frac{1}{\max(M, N)} \sum_{(i,j) \in \mathcal{M}^*} R_{ij}.$$

This formulation ensures that the reward signal captures both overlap accuracy and geometric consistency while providing stable supervision during training.

C.4 Motion Consistency Precision (MCP) Reward

While spatial rewards such as IoU evaluate frame-wise localization accuracy, they do not explicitly enforce temporal consistency across consecutive frames. To address this limitation, we introduce the **Motion Consistency Precision (MCP)** reward, which encourages predicted bounding boxes to follow the motion trajectory of the ground-truth object across time.

Specifically, the MCP reward evaluates three aspects of motion:

- **Direction alignment** between predicted and ground-truth motion
- **Speed consistency** of object movement
- **Anti-static penalty** to prevent degenerate stationary predictions

Let

$$B_{t-1}^{gt}, B_t^{gt}, B_t^{pred}$$

denote the ground-truth bounding boxes at frames $t - 1$ and t , and the predicted bounding box at frame t respectively.

All bounding boxes are represented using the $[x1, y1, x2, y2]$ coordinate format

$$B_t = (x_{1,t}, y_{1,t}, x_{2,t}, y_{2,t})$$

where $(x_{1,t}, y_{1,t})$ and $(x_{2,t}, y_{2,t})$ denote the top-left and bottom-right corners.

Bounding Box Centers To model object motion, we first compute the center of each bounding box

$$c_t = \left(\frac{x_{1,t} + x_{2,t}}{2}, \frac{y_{1,t} + y_{2,t}}{2} \right).$$

Let c_t^{gt} and c_t^{pred} denote the centers of the ground-truth and predicted bounding boxes.

Motion Vectors The ground-truth motion vector is defined as

$$\Delta \mathbf{g}_t = c_t^{gt} - c_{t-1}^{gt}.$$

Similarly, the predicted motion vector is

$$\Delta \mathbf{p}_t = c_t^{pred} - c_{t-1}^{gt}.$$

The corresponding motion magnitudes are

$$v_t^{gt} = \|\Delta \mathbf{g}_t\|, \quad v_t^{pred} = \|\Delta \mathbf{p}_t\|.$$

If the ground-truth motion is nearly static ($v_t^{gt} \approx 0$), motion consistency is not enforced and the reward is set to 1.

Direction Consistency Direction consistency measures alignment between predicted and ground-truth motion using cosine similarity

$$\cos \theta_t = \frac{\Delta \mathbf{p}_t \cdot \Delta \mathbf{g}_t}{\|\Delta \mathbf{p}_t\| \|\Delta \mathbf{g}_t\|}.$$

We normalize the cosine similarity to the interval $[0, 1]$

$$A_t = \frac{1 + \cos \theta_t}{2}.$$

A value close to 1 indicates strong directional agreement.

Algorithm 2 Motion Consistency Precision (MCP) Reward

Require: $B_{t-1}^{gt}, B_t^{gt}, B_t^{pred}$

1: Compute bounding box centers

$$c_{t-1}^{gt} = \left(\frac{x_{1,t-1}^{gt} + x_{2,t-1}^{gt}}{2}, \frac{y_{1,t-1}^{gt} + y_{2,t-1}^{gt}}{2} \right)$$

$$c_t^{gt} = \left(\frac{x_{1,t}^{gt} + x_{2,t}^{gt}}{2}, \frac{y_{1,t}^{gt} + y_{2,t}^{gt}}{2} \right)$$

$$c_t^{pred} = \left(\frac{x_{1,t}^{pred} + x_{2,t}^{pred}}{2}, \frac{y_{1,t}^{pred} + y_{2,t}^{pred}}{2} \right)$$

2: Compute motion vectors

$$\Delta g = c_t^{gt} - c_{t-1}^{gt}$$

$$\Delta p = c_t^{pred} - c_{t-1}^{gt}$$

3: Compute motion magnitudes

$$v^{gt} = \|\Delta g\|, \quad v^{pred} = \|\Delta p\|$$

4: **if** $v^{gt} < \epsilon$ **then return** 1.05: **end if**

6: Compute direction consistency

$$\cos\theta = \frac{\Delta p \cdot \Delta g}{\|\Delta p\| \|\Delta g\| + \epsilon}$$

$$A = \frac{1 + \cos\theta}{2}$$

7: Compute speed consistency

$$S = \exp\left(-\frac{(v^{pred} - v^{gt})^2}{2(\alpha v^{gt})^2}\right)$$

8: Compute anti-static penalty

$$P = \begin{cases} 0.2 & \text{if } v^{pred} < 0.1 v^{gt} \\ 1.0 & \text{otherwise} \end{cases}$$

9: Compute final MCP reward

$$R_{MCP} = A \cdot S \cdot P$$

return R_{MCP}

Speed Consistency Speed consistency evaluates whether the predicted motion magnitude matches the ground-truth motion speed. This is modeled using a Gaussian penalty

$$S_t = \exp\left(-\frac{(v_t^{pred} - v_t^{gt})^2}{2(\alpha v_t^{gt})^2}\right)$$

where $\alpha \in [0.5, 1.0]$ controls tolerance to speed deviations.

Anti-Static Penalty To discourage degenerate solutions where the model predicts nearly static bounding boxes for moving objects, we introduce

$$P_t = \begin{cases} 0.2 & \text{if } v_t^{pred} < 0.1 v_t^{gt} \\ 1.0 & \text{otherwise} \end{cases}$$

Final MCP Reward The final reward combines all motion consistency components

$$R_{MCP,t} = A_t \cdot S_t \cdot P_t$$

Since each term lies in $[0, 1]$, the final MCP reward is also bounded within $[0, 1]$. Larger values indicate stronger agreement between predicted and ground-truth motion. Algorithm 2 summarizes the complete computation procedure.

D Metrics and Implementation Details

Hardware setup. All model evaluations were conducted on a single NVIDIA H100 GPU (100GB), ensuring consistent hardware conditions across experiments. During evaluation, visual inputs and corresponding queries are processed by the selected VLM agent, which produces structured outputs in a predefined JSON format.

Training hyperparameters. Table 7 summarizes the hyperparameters used to train QTrack on the RMOT26 benchmark. Due to memory constraints, training was performed using only two frames per query. Training with the full sequence length may lead to different performance characteristics.

D.1 Motion Consistency Precision (MCP)

Traditional tracking metrics primarily focus on spatial alignment (e.g., IoU) or identity preservation across frames. However, such metrics do not explicitly evaluate whether predicted trajectories follow physically consistent motion patterns over time. To address this limitation, we introduce **Motion Consistency Precision (MCP)**, a metric designed to measure the temporal coherence between predicted and ground-truth object trajectories.

MCP evaluates whether the predicted motion follows the same trajectory dynamics as the ground truth by jointly considering both the *direction* and the *speed* of motion. Intuitively, a reliable tracker should not only localize objects accurately in each frame but should also maintain motion patterns consistent with the underlying object dynamics.

Table 7: Training hyperparameters for QTrack.

Hyperparameter	Value	Hyperparameter	Value
<i>max_prompt_length</i>	1300	<i>max_response_length</i>	2000
<i>max_pixels</i>	12845056	<i>use_kl_loss</i>	true
<i>kl_loss_coef</i>	5.0e-3	<i>fsdp.param_offload</i>	false
<i>fsdp.torch_dtype</i>	null	<i>offload.param_offload</i>	true
<i>offload.optimizer_offload</i>	true	<i>rollout.n</i>	8
<i>limit_images</i>	2	<i>learning_rate</i>	1.0e-6
<i>weight_decay</i>	1.0e-2	<i>max_grad_norm</i>	1.0
<i>global_batch_size</i>	1	<i>adv_estimator</i>	grpo
<i>kl_coef</i>	0.0	<i>kl_penalty</i>	kl
<i>tapo_strategy</i>	freeze	<i>tapo_keep_prob</i>	0.7
<i>tapo_interval</i>	2	<i>tapo_kl_weight</i>	0.1
<i>rollout_batch_size</i>	1	<i>temperature</i>	1.0
<i>tensor_parallel_size</i>	1	<i>total_episodes</i>	4
<i>n_gpus_per_node</i>	1		

Bounding box representation. For each frame t , an object is represented by a bounding box

$$B_t = (x_t, y_t, w_t, h_t), \quad (6)$$

where (x_t, y_t) denotes the center coordinates of the bounding box, and w_t and h_t denote its width and height. Let

$$B_t^{gt} = (x_t^{gt}, y_t^{gt}, w_t^{gt}, h_t^{gt}) \quad (7)$$

denote the ground-truth bounding box, and

$$B_t^{pred} = (x_t^{pred}, y_t^{pred}, w_t^{pred}, h_t^{pred}) \quad (8)$$

denote the predicted bounding box at frame t .

Bounding box motion. The motion of an object between two consecutive frames is defined as the displacement of the bounding box center. The ground-truth and predicted motion vectors are therefore computed as

$$\Delta \mathbf{g}_t = \begin{bmatrix} x_t^{gt} - x_{t-1}^{gt} \\ y_t^{gt} - y_{t-1}^{gt} \end{bmatrix}, \quad \Delta \mathbf{p}_t = \begin{bmatrix} x_t^{pred} - x_{t-1}^{pred} \\ y_t^{pred} - y_{t-1}^{pred} \end{bmatrix}. \quad (9)$$

These vectors capture the instantaneous motion of the object in the image plane.

Direction consistency. To evaluate whether the predicted trajectory follows the same motion direction as the ground truth, we compute the cosine similarity between the predicted and ground-truth motion vectors:

$$\cos \theta_t = \frac{\Delta \mathbf{p}_t \cdot \Delta \mathbf{g}_t}{\|\Delta \mathbf{p}_t\| \|\Delta \mathbf{g}_t\|}. \quad (10)$$

The direction consistency score is then defined as

$$A_t = \frac{1 + \cos \theta_t}{2}, \quad (11)$$

which maps the cosine similarity to the interval $[0, 1]$. Values close to 1 indicate strong alignment between predicted and ground-truth motion directions, whereas lower values indicate directional disagreement.

Speed consistency. In addition to directional alignment, MCP evaluates whether the magnitude of the predicted motion matches the ground-truth motion speed. The corresponding motion magnitudes are

$$v_t^{pred} = \|\Delta \mathbf{p}_t\|, \quad v_t^{gt} = \|\Delta \mathbf{g}_t\|. \quad (12)$$

Speed consistency is modeled using a Gaussian penalty that measures the deviation between predicted and ground-truth speeds:

$$S_t = \exp\left(-\frac{(v_t^{pred} - v_t^{gt})^2}{2(\alpha v_t^{gt})^2}\right). \quad (13)$$

The parameter α controls the tolerance to speed deviations. Smaller values enforce stricter speed matching, while larger values allow more flexibility. In our experiments, we set $\alpha = 0.9$ to provide robustness against small motion variations arising from annotation noise, frame discretization, and minor localization errors.

Motion Consistency Precision. The frame-level motion consistency score is defined as the product of direction and speed consistency:

$$\text{MCP}_t = A_t \cdot S_t. \quad (14)$$

For a sequence of T frames, the overall Motion Consistency Precision is computed as

$$\text{MCP} = \frac{1}{T-1} \sum_{t=2}^T \text{MCP}_t. \quad (15)$$

By construction, MCP lies within the range $[0, 1]$, where higher values indicate stronger agreement between predicted and ground-truth motion trajectories. Unlike purely spatial metrics, MCP explicitly measures the *temporal realism* of object motion, making it particularly suitable for evaluating tracking systems that must maintain coherent trajectories across time.

Table 8: Comparison of VLLM models after fine-tuning.

Model	Params	MCP \uparrow	MOTP \uparrow	MOTA \uparrow	NDE \downarrow
Qwen 2.5 VL Instruct [56]	3B	0.14	0.76	-0.51	3.41
Gemma3 [55]	4B	0.18	0.73	-0.16	0.95
Visionreasoner [35]	3B	<u>0.22</u>	0.65	<u>0.01</u>	<u>0.76</u>
QTrack (Ours)	3B	0.30	<u>0.75</u>	0.21	0.39

E Evaluation Protocol for Traditional MOT Comparison

To compare **QTrack** with traditional multi-object tracking (MOT) methods, we design a query-based evaluation protocol derived from standard MOT benchmarks. Specifically, we use sequences from the MOT17 [40] and DanceTrack [52] datasets, adapting them to reflect the query-driven nature of our task. Traditional MOT benchmarks evaluate trackers that detect and track *all* objects across an entire video. In contrast, **QTrack** is designed to track only objects specified by a natural-language query. Direct evaluation on full MOT videos would therefore be inconsistent with the intended task. To address this mismatch, we construct *query-specific tracking segments* from benchmark sequences so that both **QTrack** and conventional trackers can be evaluated under comparable conditions. For each sequence, we first select a reference frame containing the target object and generate a natural-language query describing that object. Starting from this reference frame, the tracker is required to follow only the queried target across subsequent frames. The predicted trajectories are then converted to the standard MOT annotation format, enabling the computation of common tracking metrics such as HOTA, MOTA, and MOTP.

This protocol allows **QTrack** to be evaluated on widely used MOT datasets while preserving the query-based nature of the task. At the same time, it enables meaningful comparison with traditional trackers by isolating the trajectory of the queried object within a multi-object scene. Notably, this evaluation setting introduces a stricter requirement for **QTrack**. Instead of relying on global associations among all objects in the scene, the tracker must reason about the identity of the queried target and maintain its trajectory over time. Despite this constraint, **QTrack** achieves competitive or superior performance on standard MOT metrics, demonstrating that query-aware reasoning can improve robustness in complex tracking scenarios. Overall, this protocol bridges traditional MOT evaluation with query-based tracking, enabling fair and practical comparisons between the two paradigms.

F Comparison with Fine-Tuned Models

Table 8 evaluates fine-tuned VLLMs under identical training settings. QTrack achieves the highest MCP (0.30), highest MOTA (0.21), and lowest NDE (0.39),

highlighting the importance of reward design and temporal regularization beyond supervised fine-tuning.



"Observe how the person wearing a blue shirt and carrying a black bag moves through the mall, keeping an eye on his trajectory as he walk past the LG OLED TV advertisement."

Fig. 7: Qualitative comparison for single-object tracking across multiple frames. **QTrack** produces more accurate and stable bounding boxes over time, while baseline VLLM models often exhibit drifting or inconsistent localization as the sequence progresses.

G Additional Qualitative Results

We present additional qualitative comparisons to further analyze the behavior of **QTrack** under different tracking scenarios. Figures 7 and 8 compare the predictions of several VLLM-based baselines with our proposed method across multiple frames. As illustrated, **QTrack** produces more stable and accurate trajectories

across time, particularly in challenging situations involving motion, occlusion, and appearance similarity. In contrast, baseline models often exhibit drifting predictions or inconsistent localization across frames.

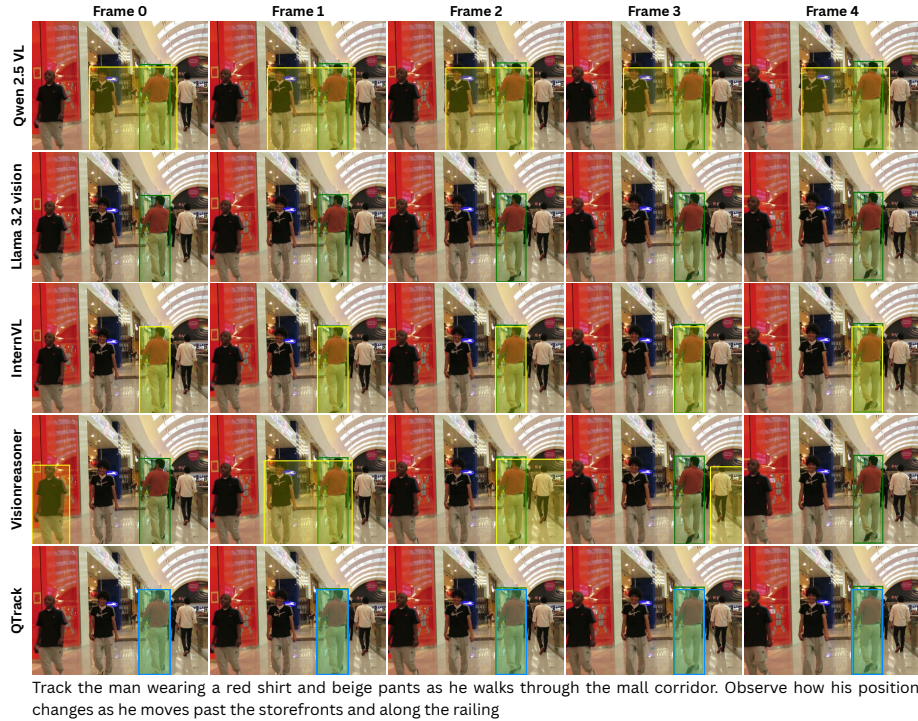


Fig. 8: Additional qualitative comparison of different VLLM models on challenging tracking scenarios. Our method demonstrates stronger temporal consistency and better object localization compared to baseline models.

Figure 9 investigates the impact of providing an initial bounding box in the reference frame. We evaluate two settings: (1) the model receives both a natural-language query and the initial bounding box of the target object, and (2) the model receives only the natural-language query without any spatial initialization. When the initial bounding box is provided, the model is able to reliably maintain the trajectory of the queried object across subsequent frames. However, when the model relies solely on the textual query, it occasionally struggles to precisely localize the target object in the first frame. This highlights an important limitation of current vision-language models: while they can reason about object descriptions, precise spatial grounding from language alone remains challenging in complex scenes.

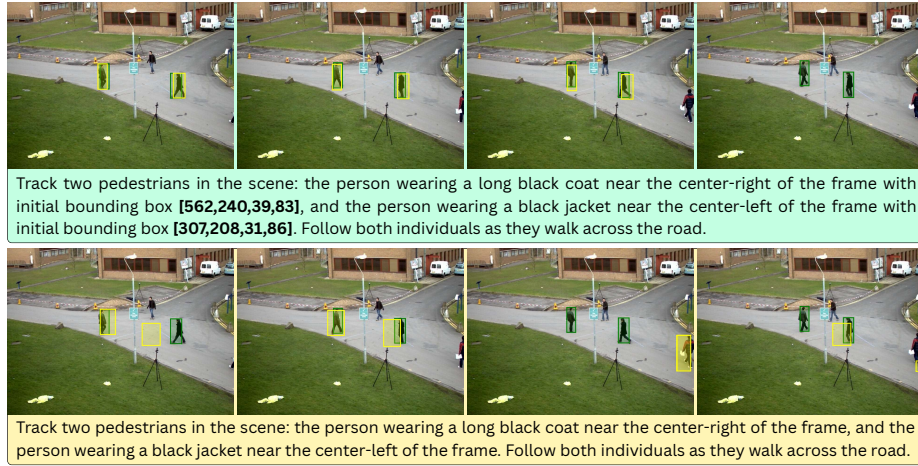


Fig. 9: Effect of spatial initialization. Tracking is reliable with an initial bounding box, but localization becomes difficult when relying solely on language queries.

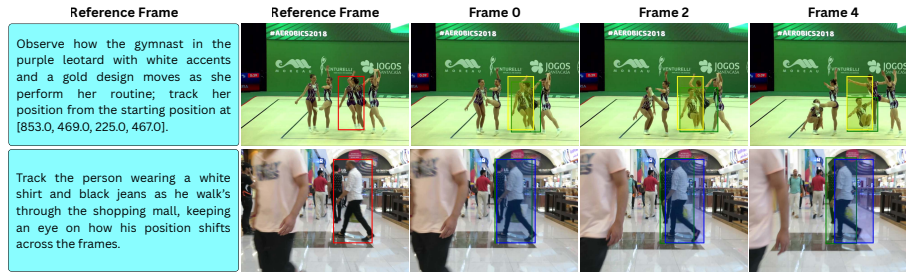


Fig. 10: This figure shows failure cases of QTrack, we can see that for some sequences QTrack is unable to predict next bounding box for frames, it repeatedly predicts the same initial bounding box for all future frames.

H Failure Cases

Figure 10, shows failure cases of QTrack, we can see that for some sequences QTrack is unable to predict next bounding box for frames, it repeatedly predicts the same initial bounding box for all future frames.

I Prompt Templates for Baseline Models

To ensure a fair comparison, all baseline models are evaluated using the same input information and prompt structure.

Input format. Each model receives the following inputs:

- Video frames from the sequence
- A natural-language query describing the target object

- A reference bounding box indicating the initial location of the object in the reference frame

Prompt template. We use a unified prompt template for all baseline models. The template instructs the model to track the queried object across the provided video frames and output the predicted bounding boxes in a structured JSON format.

Prompt Template

```
{textual_query}

Initially, object {obj_id} is located at {initial_bbox}
in the reference image.

The following images correspond to consecutive
frames of a video.

Please output the bounding box for the object in
each frame using the following format:

[{"frame": N, "bbox": [x1, y1, x2, y2]}, ...]

Do not include any additional text.
```

This prompt ensures that all models receive identical instructions and output constraints. By enforcing a structured JSON response format, we simplify downstream parsing and ensure consistent evaluation across different baseline models.